Appl. Phys. B 52, 361–366 (1991)

Applied Physics B Photophysics and Laser Chemistry

© Springer-Verlag 1991

On the Transport of Activated Particles by Flow and Diffusion

G. Schulz and M. Simon

Universität des Saarlandes, FB Exp. Physik, W-6600 Saarbrücken, Fed. Rep. Germany

Received 25 February 1991/Accepted 20 April 1991

Abstract. It will be shown, how the spatial decay of active molecules – excited electronically or activated otherwise (e.g., chemical processes) is determined by diffusion and flow as well as by the intrinsic molecular constant. The exact analysis in cylindric geometry leads to a set of unique solutions, which in lowest order are characterized by a weak gradient of the particle concentration at the wall and a pronounced kernel in the center of the tube. In special cases there exists a simple but powerfull expansion of any distribution in the source, which are very similar to Fourier-Bessel series. The solutions in lowest order will be used to analyze the measured decay of activated oxygen in a steady stream of molecular oxygen. Since the decay constant is determined by volume deactivation and by the removal of particles at the wall, evaluation of experimental data, however, remains necessarily ambiguous.

PACS: 51.70, 82.40P

The transport of atoms or molecules with long-lived excited states in flowing media has been investigated and reviewed extensively [1, 2]. Corresponding experiments were often evaluated by means of theoretical derivations which are confined to special ranges of pressure and particle concentration [3] or which are only approximately valid [4–6]. It will be shown that approximations are not necessary at all, because unique and comprehensive solutions exist. The phenomenon is governed by at least three effects: 1) the motion of the particles, i.e. flow and diffusion of the participating species, 2) the collisional interaction of particles in the bulk and at the wall of the cavity, and 3) absorption and reemission of radiation, which may additionally fill or deplete the excited states [7]. These effects play an important role in streaming plasmas, used for the etching and deposition applciations and in the corona of high-frequency flames and may also have some influence on the energy balance of plasma jets. In some cases the phenomena may be separated experimentally. This paper discusses the radiation transport of the excited or activated particles by convection, diffusion and collisional interaction alone. The superposition of absorption and reemission on the particle-motion will be described in a forthcoming paper.

If nitrous oxide NO is added to a low concentration of oxygen in a steady stream of a rare gas, activated e.g. by a radio-frequency discharge, one observes the prompt emission of a greenish-yellow radiation in the spectral region from 400 nm to more than 700 nm which is typical for the well-known airglow. The phenomenon persists even when the nitrous oxide is added in a region far from the source of activation where no spontaneous emission is present (Fig. 1). This indicates a very long apparent lifetime of the active species. If we assume that the radiation is due to some first-order reaction of oxygen with NO or to the direct energy transfer from activated oxygen to NO, the intensity of the radiation will be proportional to the concentration of particles. Hence, the added NO merely acts as a target as in the well-known beam foil method [8].

In a series of experiments a thin capillary was used to introduce NO into the gas flow to minimize perturbations. The optical intensity from a $4 \times 4\,\mathrm{mm}^2$ region immediately behind the inlet was detected by a microprocessor controlled photoncounting system, which has

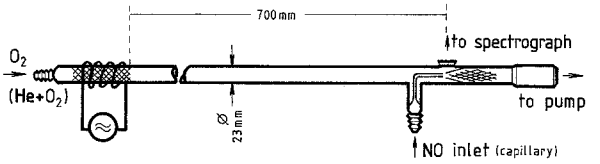

Fig. 1. Experimental setup for the preparation of active oxygen by a radio frequency discharge at 62 MHz. Direct interaction of oxygen with NO at a pressure of 1 mbar

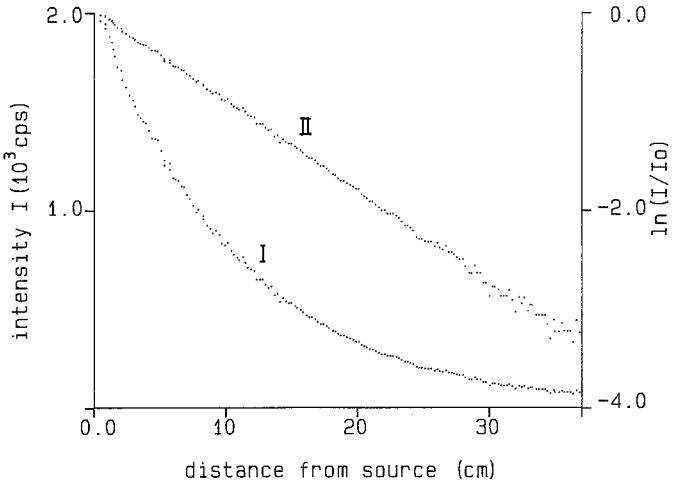

Fig. 2. Radiation from the interaction zone of activated oxygen and nitrous oxide as a function of the distance behind the source of activation, at a pressure of 1 mbar: *I* Multichannel signal at rates of 10^3 counts per second. *II* Semilogarithmic plot of *I* giving the decay constant $\lambda_{exp}=0.094\ cm^{-1}$

already been described in a previous publication [9]. The velocity of the streaming gas was so adjusted that obviously no backdiffusion of radiating particles occured. The monochromator was set to the wavelength of maximum intensity at 560 nm with a slitwidth of 4 mm. Varying the distance between the rf source and the NO inlet by moving the induction coil of the rf source we got as a multi-channel signal curve I in Fig. 2 for the decay of activated oxygen in purified and highly dried oxygen.

The spatial decay is commonly transformed into a temporal decay by dividing the distance between the source and the point of observation by the velocity of the gas flow, i.e. by the mean velocity which only can be measured outside the tube. However, the distribution of the active particles inside the tube is not uniquely defined by the gas flow alone, because of diffusion and deactivation in the volume and at the wall of the tube. The semilogarithmic plot II of the intensity as function of the distance in Fig. 2 shows very slight deviations from linearity which indicate that a first-order process dominates the removal of activated oxygen.

The measured intensity in the target region is most likely due to the direct interaction of O atoms with the added NO molecules in a first-order reaction leading to excited NO_2^*. This process was first assumed by Gaydon [10] and affirmed by Kaufman [1]. It might be mentioned that the excited NO_2^* complex can only be formed, if stabilized by threebody collisions. The extremely slow decay of the O concentration cannot be explained by the simple interaction of O atoms with O atoms, i.e. by recombination, because recombination is a second-order reaction and therefore very fast. Tentatively it may be assumed that the long lifetime of the O atoms is due to some activation, which inhibits direct recombination, but which does not hinder the direct interaction of O with NO. Another spectroscopic experiment in crossed beams of high-frequency activated oxygen and NO at a pressure as low as 10^{-4} mbar prevealed exactly the same characteristic radiation between 400 and 700 nm. It should be noted that under these conditions threebody-collisions do not occur [11]. However, even in case of the crossed beams set-up the activated oxygen has to be prepared at high pressures in the presence of a high-frequency discharge and then transported into the low-pressure reaction chamber through a small nozzle. This indicates that the production of O atoms and their activation occurs stepwise. Further evaluation of experimental results requires a rigorous theoretical analysis of how the phenomenological constants of diffusion and gas flow are connected with the intrinsic molecular characteristics.

1. Analysis

For the given experimental setup the behaviour of the activated particles has to be described by the continuity equation in cylindric coordinates:

$$D\Delta n(r,z)-v_z(r)\partial n(r,z)/\partial z-A_{nm}n(r,z)=0, \tag{1}$$

where $n(r,z)$ stands for the particle concentration as a function of the radial and the axial coordinate r and z, respectively, and $v_z(r)$ denotes the velocity in z-direction as a function of the radial coordinate r alone. A_{nm} is the coefficient of volume deactivation probability (Einstein-coefficient for the transition from state m to n). It may be assigned to the mean lifetime of the activated particles by $\tau=1/A_{nm}$. The diffusion-constant of atomic oxygen in molecular oxygen is denoted by D. Diffusion cannot be neglected where viscous flow occurs and vice versa, since both transport phenomena are based on the same source, viz. the thermal agitation of particles. Laminar flow in cylindric coordinates is described by the law of Hagen-Poiseuille:

$$v_z(r)=2\bar{v}(1-r^2/r_0^2), \tag{2}$$

where $\bar{v}$ denotes the mean velocity in z direction, and r_0 is the radius of the tube. The mean velocity can be determined by measuring the gas flow outside the tube, i.e. without any knowledge of the molecular viscosity. The coefficient $A_{n,m}$ and the diffusion constant D, however, are intrinsic molecular constants, one of which must be known in order to evaluate experimental results.

As in the case of pure diffusion, when $v_z(r)=0$, the differential equation (1) is separabel in r and z and yields the separation ansatz

$$n(r,z)=y(r)\exp(-\lambda z) \tag{3}$$

in which – on physical grounds – only the negative sign in the exponential is acceptable. Now the substitution

$$\varrho=r(\lambda^2+2\lambda\bar{v}/D-A_{n,m}/D)^{1/2} \tag{4}$$

and the abbreviation

$$\beta=(2\lambda\bar{v}/D)/[r_0^2(\lambda^2 2\lambda\bar{v}/D-A_{n,m}/D)^2] \tag{5}$$

lead to a differential equation with only one parameter β:

$$d^2y/d\varrho^2+1/\varrho dy/d\varrho+(1-\beta\varrho^2)y=0. \tag{6}$$

The solutions of this second-order differential equation are determined by the boundary condition at the wall of

the tube, at $r=r_0$, and by the distribution of $n=n(r,0)$ in a given plane, say in the source at $z=0$. Equation (6) includes the case of pure diffusion (called the eigenvalue problem of diffusion in cylindric geometry), if one sets $\beta=0$. In that special and well-known case the Bessel function $J_0(\varrho)$ of the first kind and zero order is solution of (6). The boundary condition $n(r_0,z)=0$ can be fulfilled by $J_0(\varrho)$, running from $\varrho=0$ to any one of the zeros ϱ_ν of the Bessel function. Because every function (which fulfils the Dirichlet condition) can be represented by series of Bessel functions, the second condition can be satisfied by the superposition of solutions in the form of Fourier-Bessel series [12]

$$n(r,z)=\sum_{\nu}^{\infty} b_\nu J_0(\varrho_\nu\xi)\exp(-\lambda_\nu z), \tag{7}$$

where ξ runs from 0 to 1 as r goes from 0 to r_0 and the values of λ_ν are uniquely determined by the zeros of J_0, inserted into (4). The λ_ν are called the eigenvalues of the (entire) set of eigenfunctions $y_\nu(\xi)=J_0(\varrho_\nu\xi)$. The coefficients are then given [12, 13] by:

$$b_\nu=(2/y_\nu'^2)\int_0^1 n(r_0\xi,0)y_\nu(\xi)\xi d\xi, \tag{8}$$

where y'_ν denotes the first derivative of J_0 at ϱ_ν. It should be mentioned that an appropriate representation exists even when the boundary condition is $n(r_0,z)\neq 0$ [13]. But it should also be mentioned that the higher-order λ_ν are so much greater than λ_0, corresponding to $\varrho_0=2.4048$, that in many practical cases, at some distance from the source, only the solution $y_0(\xi)=J_0(\varrho_0\xi)\exp(-\lambda_0 z)$ persists.

In the actual case with $v_z(r)\neq 0$, i.e. with β according to (5), the analytical solution of the complete equation (6) is given by

$$y(\varrho)=\sum_{\mu} a_\mu \varrho^{2\mu} \tag{9}$$

with $a_0=1.0$, $a_1=-0.25a_0$

$$a_\mu=-\frac{1}{(2\mu)^2}(a_{\mu-1}-\beta a_{\mu-2}).$$

To prove that this solution is analytical, absolutely convergent and therefore unique[1] in the whole region $(0,\infty)$, we build at first

$$\frac{a_m}{a_{m-1}}=\frac{-1}{(2m)^2}\left(1-\frac{\beta}{a_{m-1}/a_{m-2}}\right). \tag{10}$$

By continuously inserting a_{m-1}/a_{m-2} we obtain the continuous fraction [15]

$$\frac{a_m}{a_{m-1}}=\frac{-1}{(2m)^2}\left(1+\frac{\beta 2^2(m-2)^2|}{|1+}\right.$$
$$\left.+\frac{\beta 2^2(m-2)^2|}{|1+}+\frac{\beta 2^2(m-m+1)^2|}{|1}\right). \tag{11}$$

[1] By another method Aris [14] obtained solutions in totally different form which, of course, should be reducible to the analytical form given here

Theory of continuous fraction [16] yields:

$$\left|\frac{a_m}{a_{m-1}}\right|=\frac{M}{2^2 m} \text{ with a positiv constant } 0<M\leqq 1$$
$$\text{for all } \beta 2^2\leqq 1. \tag{12}$$

Thus the absolute ratio of successive coefficients goes to zero as m tends to infinity. In the special case $\beta 2^2=1$, i.e., $\beta=0.25$, one obtains $M=1$ and the power series (9) becomes exactly

$$y=\sum_{\mu}(-1)^\mu\frac{(\varrho/2)^{2\mu}}{\mu!}=\exp[-(\varrho/2)^2], \tag{13}$$

which at once can be affirmed by inserting (13) into (6) with $\beta=1/4$. But a physically meaningful solution must have at least one zero in order to fulfil the boundary condition. For comparison, in Fig. 3 solutions are shown between $r=0$ and $r=r_0$ – where $y(\varrho_0)=0$ – for some extreme values of the parameter β: When β goes to 0, i.e. for vanishing velocity v_z, we obtain from (6) automatically the Bessel function J_0, as shown in curve I. With increasing β up to $\beta=0.2499995$, which gives $\varrho_0=6.28$ and which would correspond to very high velocities, the solutions are characterized by a very weak gradient of the particle concentration at the wall, which implies a pronounced kernel in the center of the tube, as shown by curve II. For even greater β one can only construct solutions with $n(r_0,z)>0$ and $(\partial n/\partial r)_{r_0}\sim 0$, as shown by III in Fig. 3. But in this case of purly mathematical interest, one has $1<M$, which reduces the circle of convergence drastically. Therefore curve III has only been drawn from $\varrho=0$ to the point ϱ_0 where $\partial y/\partial\varrho=0$.

In the actual case too the decay constants λ_ν are uniquely determined by the zeros ϱ_ν of the solutions $y(\varrho)$ in (9):

$$\lambda_\nu=[(\bar v/D)^2+(\varrho_\nu/r_0)^2+A_{nm}/D]^{1/2}-\bar v/D, \tag{14}$$

and so β_ν is determined by λ_ν, when the parameters $\bar v/D$ and A_{nm}/D are given. Thus the physically meaningful solutions have to be determined in a self-consistent way by an iteration process. One firstly chooses some plausible

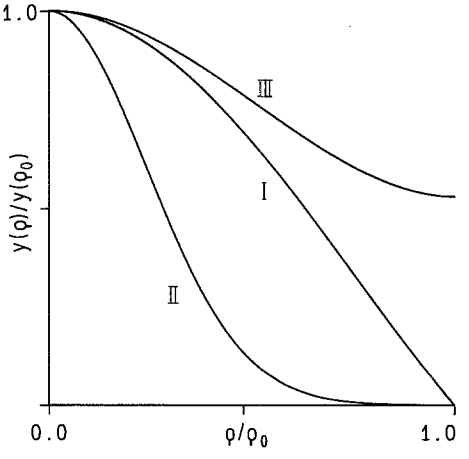

Fig. 3. Typical solutions of the transport equation for various values of the parameter β. *I*: $\beta=0\rightarrow\varrho_0=2.41$ Bessel function J_0, $\bar v/D=0$, *II*: $\beta=0.2599995\rightarrow\varrho_0=6.26$ profil with $y(\varrho_0)=0$, $\bar v/D\gg 1$; *III*: $\beta=0.5\rightarrow\varrho_0=2.13$ for vanishing $\partial y(\varrho)/\partial\varrho$ and $y(\varrho)\neq 0$

value for $\varrho_\nu^{(1)}$, say the appropriate zero of the Bessel function and determines the corresponding λ_ν by (14) and β_ν by (5). Now calculating $y(\varrho)$ in fine steps one will obtain perhaps another zero $\varrho_\nu^{(1)'}$ and start the procedure again with $\varrho_\nu^{(2)}=\frac{1}{2}(\varrho_\nu^{(1)}+\varrho_\nu^{(1)'})$, simultaneously refining the step-width. The programmed procedure should be terminated if $|\varrho^{(n+1)}-\varrho^{(n)}|\leqq\varepsilon$ with some small value of ε. We found $\varepsilon=10^{-5}$ sufficiently small for all practical purposes.

The solutions between $\varrho=0$ and ϱ_0 only describe the steady state at some distance beyond the source of activation. Immediately behind the source solutions of higher-order zeros will persist, although more rapidly decaying Furthermore, the series in (5) are not well conditioned for numerical evaluation. If one looks for an expansion of (5) as a function of the parameter β, however, one obtains

$$y_\nu(\varrho)=\sum_{\mu=0}^{\infty}\frac{g_\mu(\varrho)}{\mu!}(\varrho^4\beta_\nu)^\mu, \tag{15}$$

where $g_0(\varrho)=J_0(\varrho)$ is the Bessel function of the first kind and zero order and the other auxiliary functions $g_\mu(\varrho)$ are rapidly decaying functions of ϱ, as shown in Fig. 4[2]. Successive derivation of the series (9) yields

$$g_\mu(\varrho)=\sum_{n=2\mu}^{\infty}c_{\mu,n}\varrho^{2n-4\mu} \tag{16}$$

with $c_{0,0}=1$, $c_{\mu,\mu-1}=0$, and

$$c_{\mu,n}=\frac{1}{(2n)^2}(c_{\mu,n-1}-\mu c_{\mu-1,n-2}). \tag{17}$$

Because the parameter β includes the ν^{th} zero of the solution in the form ϱ_ν^4, we arrive at $(\varrho^4\beta_\nu)=\kappa_\nu^\mu\xi^{4\mu}$ with $\xi=\varrho/\varrho_\nu$ i.e. $0<\xi<1$, which yields an excellent convergence even for solutions with higher-order zeros, up to the order 9. The results of the calculations are shown in Table 1 for some experimentally interesting values of $\bar{v}/D$ and A_{nm}/D. The new auxiliary constant κ can be written $\kappa_\nu=2\lambda_\nu r_0^2\bar{v}/D$ which together with (14) at extremely high values of $\bar{v}/D$ approximately becomes $\kappa_\nu\sim\varrho_\nu^2$. When the Bessel function describes the molecular transport at vanishing flow, the general solution (9 or 15) yields a description also in the other extreme case of very high velocities. If $(\bar{v}/D)^2\gg A_{nm}/D$ and $(\bar{v}/D)^2\gg(\varrho_\nu/r_0)^2$, then we obtain

$$\beta\varrho_\nu^2=1. \tag{18}$$

Quite analogous to (7) one can build the superposition of solutions

$$n(r,z)=\sum_\nu b_\nu y_\nu(\xi)\exp(-\lambda_\nu z). \tag{19}$$

In a very similar way which leads to (8) [12, 13], one finds on account of (18), at least for large $\bar{v}/D$:

$$b_\nu=(2/y_\nu'^2)\int_0^1(1-\xi^2)n(r_0\xi,0)y_\nu(\xi)\xi d\xi, \tag{20}$$

where again y_ν' denotes the first derivative of $y_\nu(\xi)$ at $\xi=1$. In case $n(r_0,z)\neq0$ the factor in front of the integral will adopt a more complicated form [13]. But Table 2 shows clearly that the decay constants $\lambda_0<\lambda_1<\ldots<\lambda_N$. Moreover, it should be mentioned, that for all values of $\bar{v}/D$ the values of β_ν becomes small and even smaller with growing ν. Only the gradient of the lowest-order solution is strongly influenced by flow at $\varrho=\varrho_\nu$, so that $y_0'\ll y_{\nu\neq0}'$. Thus here also only the solution $y_0(\xi)$ with λ_0 persist over some distance behind the source. According to the fact, that the experimental data can be described by a simple exponential we shall adopt this assumption throughout the following text.

The constant β_ν comprises all possible experimental arrangements and also all theoretical implications: If, for example, the deactivation of particles at the wall is not perfect, then the diffusional current of particles in radial direction must balance the reaction rate at the wall [4]. With the rate constant K_w we obtain:

$$-D(\partial n(r,z)/\partial r)_{r_0}=K_w n(r_0,z). \tag{21}$$

[2] The same expression can be found by the method of successive approximation

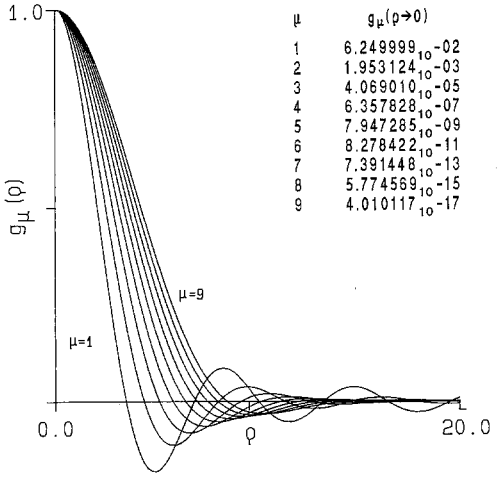

Fig. 4. Rapidly decaying auxiliary functions $g_\mu(\varrho)$ with the initial value $g_\mu(0)$ at $\varrho=0$

Table 1. First zeros ϱ_0 of the eigenfunctions for experimentally interesting values of $\bar{v}/D$ [cm^{-1}] and A_{nm}/D [cm^{-2}]. The appropriate eigenvalues λ_0 [cm^{-1}] (decay constants) are given in parentheses

Table of limiting eigenvalues ϱ_0 as functions of parameters

$\bar{v}/D$ \ A_{nm}/D	0.0	0.1	1.0	10.0	100.0
0.0	2.4048 (2.4048)	2.4048 (2.4255)	2.4048 (2.6044)	2.4048 (3.9728)	2.4048 (10.2851)
0.1	2.4258 (2.3279)	2.4261 (2.3487)	2.42759 (2.5274)	2.4398 (3.8953)	2.4947 (10.2069)
1.0	2.5553 (1.7440)	2.5570 (1.7638)	2.57074 (1.9340)	2.6746 (3.2607)	3.0859 (9.5129)
10.0	2.6984 (0.3576)	2.7030 (0.3637)	2.7422 (0.4172)	3.0729 (0.9290)	4.4337 (4.8208)
100.0	2.7044 (0.0365)	2.7089 (0.0371)	2.7499 (0.0428)	3.1027 (0.0980)	4.6980 (0.6085)

Table 2. Higher-order zeros of the eigenfunctions with various parameters $\bar{v}/D$ [cm^{-1}] and A_{nm}/D [cm^{-2}] for comparison

Table of eigenvalues ϱ_μ for selected parameters							
$\bar{v}/D$	0.0	0.1		1.0		10.0	
A_{nm}/D	0.0	0.0	0.1	0.0	0.1	0.0	0.1
ν:0	2.4048	2.4258	2.4276	2.5551	2.5707	2.6984	2.7422
1	5.5201	5.5508	5.5513	5.7912	5.7961	6.5468	6.5740
2	8.6537	8.6859	8.6861	8.9522	8.9543	10.1996	10.2155
3	11.7915	11.8242	11.8243	12.1009	12.1021	13.6841	13.6940
4	14.9309	14.9638	14.9639	15.2460	15.2468	17.0606	17.0673
5	18.0711	18.1041	18.1041	18.3898	18.3902	20.3709	20.3756
6	21.2116	21.2447	21.2447	21.5327	21.5331	23.6390	23.6425
7	24.3525	24.3856	24.3856	24.6753	24.6756	26.8791	26.8818
8	27.4935	27.5267	27.5267	27.8176	27.8178	30.0996	30.1018
9	30.6347	30.6679	30.6679	30.9597	30.9599	33.3128	33.3128

In zero order and with the substitutions of (4) this constraint can be brought into a dimensionless form:

$$-\frac{1}{y_0}\frac{\partial y_0}{\partial \varrho}\varrho_0 = r_0 K_w/D. \tag{22}$$

The rate constant K_w can be resolved into the mean thermal velocity $\bar{w}$ (in one direction $\bar{w}/4$) and the efficiency γ, which stands for the probability, that a collision with the wall will effectively remove an active particle: $K_w = \frac{1}{4}\gamma\bar{w}$. Similarly kinetic theory yields $D = \frac{1}{3}\Lambda\bar{w}$, where Λ denotes the mean free path of the particles. Thus the logarithmic derivative (22) has also the meaning:

$$-\frac{1}{y_0}\frac{\partial y_0}{\partial \varrho}\varrho_0 = \frac{3}{4}r_0\frac{\gamma}{\Lambda} \tag{23}$$

which depends on temperature only to the extent that the mean-free path Λ depends on the total particle density. Figure 5 shows a special solution and the appropriate logarithmic derivative for $r_0 = 1$ cm, $v/D = 1.0\ cm^{-1}$ and $A_{nm}/D = 0\ cm^{-2}$, which yields $\varrho_0 = 2.5549$, $\lambda_0 = 1.744\ cm^{-1}$, and $\beta_0 = 0.0818$. All values of $r_0\gamma/\Lambda$ larger than say 100 are realized in the immediate neighborhood of ϱ_0, so that the assumption $n = 0$ at $\varrho = \varrho_0$ serves as a good first approximation for great efficiencies of the removal of active particles at the wall or small mean-free paths.

If, on the other hand, the ratio $r_0 K_w/D$ becomes smaller and smaller, solutions have to be found with λ_0 or β_0, respectively, for which the negative logarithmic derivative at $\varrho = \varrho_0'$ yields the proper value of $r_0 K_w/D$ in the prescribed self consistent way. Thus we obtained the values of ϱ_0'/ϱ_0 as function of $r_0 K_w/D$ in double logarithmic coordinates (Fig. 6). The unprimed ϱ_0 stands for the limiting value, when $r_0 K_w/D$ goes to infinity, and is given in Table 1 together with the corresponding values of the decayconstant λ_0 in brackets. Curve I and IIa are valid for $A_{nm}/D = 0$ and $\bar{v}/D = 0$ and $\bar{v}/D = 1\ cm^{-1}$, respectively. Both curves become straight lines with a slope 1/2 in the limit $r_0 K_w/D \sim 0$. This derivation indicates clearly the region, where the approximations made by other researchers [3] may be valid. If, however, volume deactivation occurs, even at a very low level, $A_{nm}/D = 0.1$ and $1.0\ cm^{-2}$,

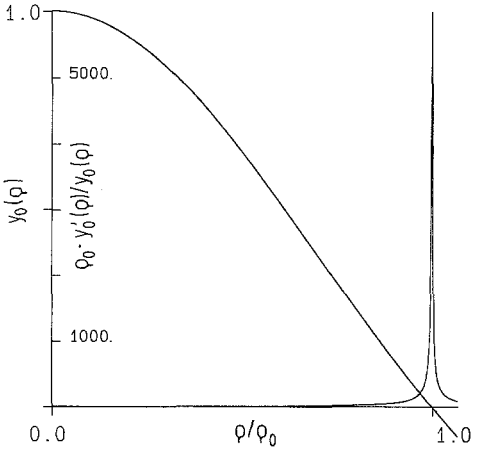

Fig. 5. Special solution of the transport equation for $r_0 = 1$ cm, $v/D = 1\ cm^{-1}$, and $A_{nm}/D = 0$, which yields $\varrho_0 = 2.5549$, $\lambda_0 = 1.744\ cm^{-1}$, and $\beta_0 = 0.0818$ and showing the typical behaviour of the logarithmic derivative $r_0 n'/n$ around r_0

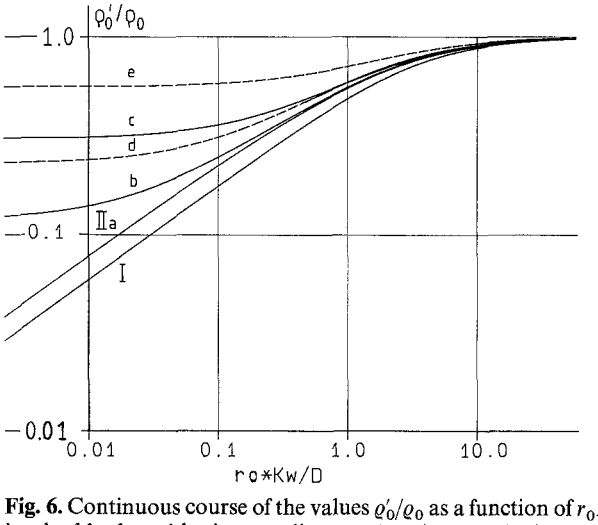

Fig. 6. Continuous course of the values ϱ_0'/ϱ_0 as a function of $r_0 K_w/D$ in double logarithmic coordinates: *I*: $\bar{v}/D = 0$, $A_{nm}/D = 0$, pure diffusion without volume deactivation. *IIa*: $\bar{v}/D = 1\ cm^{-1}$, $A_{nm}/D = 0$, slope tends also to 1/2 if $r_0 K_w/D \to 0$. *b*: $\bar{v}/D = 1\ cm^{-1}$, $A_{nm}/D = 0.1\ cm^{-2}$. *c*: $\bar{v}/D = 1\ cm^{-1}$, $A_{nm}/D = 1.0\ cm^{-2}$ limiting values if $r_0 K_w/D \to 0$: *d* and *e* corresponding to *b* and *c* with $r_0 = 2.0$ cm

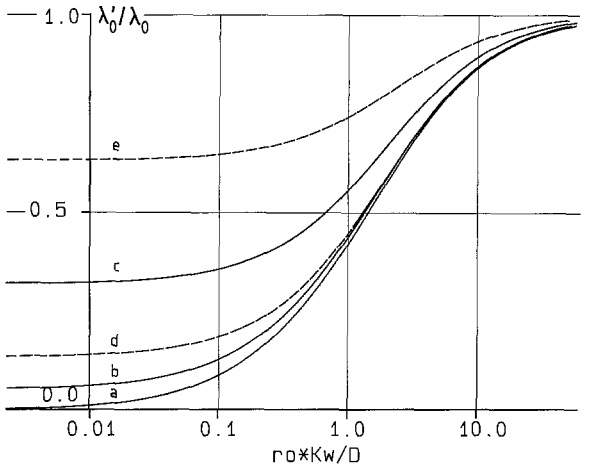

Fig. 7. Decay constants λ_0'/λ_0 corresponding to Fig. 6 in semi-logarithmic coordinates

then the simple linear relation between the roots and the wall reaction rate is broken up and ϱ_0'/ϱ_0 goes to a nearly constant value at comparably low r_0K_w/D, as shown by curve b and c in Fig. 6. The corresponding curves a–c of the decay constant λ_0'/λ_0 are drawn in Fig. 7 in semi-logarithmic coordinates. The limiting value of the decay constant λ_0 at low r_0K_w/D and finite A_{nm}/D corresponds to a limiting profile of the particle concentration, which under these conditions cannot become "flat", or in any way homogeneous over the radius of the tube. As shown in Figs. 6 and 7 by the curves in broken lines, growing radius r_0 of the tube enhances the effect of volume deactivation and deminuishes the influence of the reaction or deactivation at the wall (besides an overall shift to lower K_w/D). But without further experimental evidences it seems impossible to distinguish between the two effects and their influence on λ_0.

2. Results and Conclusion

In our experiments the gas flow was controlled by a flowmeter and the velocity exactly determined by measuring the depletion of a given volume in time. So we got: $\bar{v}=253\pm0.03$ cm/s. For the diffusion of O in O_2 at 273 K and 1 mbar pressure we obtain from literature $D=176\ \mathrm{cm^2/s}$ [18]. Therefore, the experimentally determined parameter is $\bar{v}/D=1.44\ \mathrm{cm^{-1}}$ and the data in Fig. 2 yield the decay constant $\lambda_{exp}=0.094\ \mathrm{cm^{-1}}$. Thus we obtain according to (14):

$$(\varrho_0'/r_0)^2+A_{nm}/D=0.27. \tag{24}$$

For $r_0=1.0$ cm and with the additional assumption $A_{nm}/D=0$ one obtains $\varrho_0'=0.52$ which theoretically can be achieved with $r_0K_w/D=0.072$. But with $A_{nm}/D\neq0$ also valid solutions exist, which correspond to lower values of ϱ_0' and also lower values of r_0K_w/D, until at $A_{nm}/D=0.14$ the limiting value $\varrho_0'=0.36$, according to $r_0K_w/D=0.001$, is reached. Larger values of A_{nm}/D lead theoretically to values of ϱ_0', which are incompatible with the experimental result in (24). At this relatively low value of r_0K_w/D, volume deactivation, especially in the slowly moving parts of the Hagen-Poiseuille flow, becomes dominant and forms together with diffusion and flow a concentration profile with nonvanishing particle concentration and a very little gradient at the wall. At even lower values of r_0K_w/D wall effects have no more significant influence on the decay constant. On the other hand, ϱ_0' cannot be cancelled at all, because every particle produced in the source can reach the wall and interact with it more than once. Since A_{nm}/D can be written: $A_{nm}/D=1/D\tau$ and the mean lifetime τ is likewise the migration time of the diffusing particles, we get from kinetic theory: $2D\tau=\langle\delta^2\rangle$, where δ denotes the root-mean-square distance. Hence we obtain for the limiting value $\sqrt{\langle\delta^2\rangle}=3.77$ cm, which is much larger than the radius of the tube $r_0=1.0$ cm. Thus in the region $A_{nm}/D=0.0$ to $0.14\ \mathrm{cm^{-2}}$ the evaluation of experimental results remains ambiguous.

Shifting the NO inlet to the wall, we observed, that the intensity from the target region diminishes markedly but does not vanish near the wall. So we must conclude, that the deactivation occurs at the wall as well as in the volume, but the experimental facts are not sufficient to remove the ambiguity.

Acknowledgements. The authors wish to thank Prof. Dr. K. Becker, City University of New York, for many helpful advices and are grateful to the „Deutsche Forschungsgemeinschaft" for supporting this work.

References

1. F. Kaufman: *Progress in Reaction Kinetics* (Pergamon, New York 1961) Vol. 1, pp. 11–13
2. E.E. Ferguson, F.C. Fehsenfeld, A.L. Schmeltekopf: Adv. At. Mol. Phys. **5**, 1–55 (1969)
3. W.W. Smith: J. Chem. Phys. **11**, 110–125 (1943)
4. R.E. Walker: Phys. Fluids **4**, 1211–1216 (1961)
5. P.J. Ogren: J. Phys. Chem. **79**, 1749–1752 (1975)
6. R.V. Poirier, R.W. Carr: J. Phys. Chem. **75**, 1593–1501 (1971)
7. G. Schulz, H.J. Gutjahr: Z. Angew. Phys. **29**, 26–34 (1970)
8. S. Bashkin (ed.): *Beam Foil Spectroscopy*, Topics Curr. Phys. 1 (Springer, Berlin, Heidelberg 1976)
9. K. Becker, B. Stumpf, G. Schulz: Chem. Phys. **53**, 31–38 (1980)
10. A.G. Gayson: Proc. Soc. A **183**, 111–123 (1944)
11. G. Schulz, M. Simon: Third European Conf. on Atomic and Molecular Phys., Bordeaux, ed. by A. Salin (1989) Vol. 2, p. 448
12. G.N. Watson: *A Treatise on the Theory of Bessel Functions*, 2nd ed. (Cambridge Univ. Press, Cambridge 1962)
13. Ph. Frank, R. v. Mieses: *Differential- und Integralrechnung I* (Dover, New York 1961) Chap. VIII, p. 3.7
14. R. Aris: Proc. R. Soc. A **235**, 111–123 (1956)
15. M. Abramovitz, I.A. Stegum: *Handbook of Mathematical Functions* (Dover, New York 1972)
16. R. Sauer, I. Szabo: *Mathematische Hilfsmittel des Ingenieurs III* (Springer, Berlin, Heidelberg) Chap. II, p. 4
17. E.L. Ince: *Ordinary Differential Equations* (Dover, New York 1956)
18. T.R. Marero, E.A. Mason: J. Phys. Chem. Ref. Data Vol. 1, No. 1 (1972)